Effect of Al$_2$O$_3$ on the viscosity of CaO–SiO$_2$–Al$_2$O$_3$–MgO–Cr$_2$O$_3$ slags

Chen-yang Xu[1], *Cui Wang*[2], *Ren-ze Xu*[1], *Jian-liang Zhang*[1,2], *and Ke-xin Jiao*[1]

1) School of Metallurgical and Ecological Engineering, University of Science and Technology Beijing, Beijing 100083, China
2) State Key Laboratory of Advanced Metallurgy, University of Science and Technology Beijing, Beijing 100083, China
(Received: 4 June 2020; revised: 3 September 2020; accepted: 4 September 2020)

Abstract: We investigated the effect of Al$_2$O$_3$ content on the viscosity of CaO–SiO$_2$–Al$_2$O$_3$–8wt%MgO–1wt%Cr$_2$O$_3$ (mass ratio of CaO/SiO$_2$ is 1.0, and Al$_2$O$_3$ content is 17wt%–29wt%) slags. The results show that the viscosity of the slag increases gradually with increases in the Al$_2$O$_3$ content in the range of 17wt% to 29wt% due to the role of Al$_2$O$_3$ as a network former in the polymerization of the aluminosilicate structure of the slag. With increases in the Al$_2$O$_3$ content from 17wt% to 29wt%, the apparent activation energy of the slags also increases from 180.85 to 210.23 kJ/mol, which is consistent with the variation in the critical temperature. The Fourier-transform infrared spectra indicate that the degree of polymerization of this slag is increased by the addition of Al$_2$O$_3$. The application of Iida's model for predicting the slag viscosity in the presence of Cr$_2$O$_3$ indicates that the calculated viscosity values fit well with the measured values when both the temperature and Al$_2$O$_3$ content are at relatively low levels, i.e., the temperature range of 1673 to 1803 K and the Al$_2$O$_3$ content range of 17wt%–29wt% in CaO–SiO$_2$–Al$_2$O$_3$–8wt%MgO–1wt%Cr$_2$O$_3$ slag.

Keywords: slag; viscosity; high aluminium oxide; apparent activation energy; structure; viscosity prediction

1. Introduction

As a strategic element, nickel plays an important role in economic development. Nickel is mainly present in nickel sulfide ore and laterite nickel ore, most of which is obtained from nickel sulfide ore. With the current shortage of nickel sulfide ore, the exploration and utilization of laterite nickel ore has boomed [1–2]. The processing technologies of laterite nickel ore are roughly divided into two classes: pyrometallurgical and hydrometallurgical processes. The pyrometallurgical process is the main process used to extract nickel resulted from the as yet immature hydrometallurgical process. Smelting laterite nickel ore in a blast furnace is a pyrometallurgical process independently developed in China [3]. Laterite ore is a low-grade composite iron ore containing multiple valuable elements such as Ni, Fe, Cr, and Co. Generally, the mass fraction of nickel is less than 2.8%, while that of iron varies from 9wt% to 50wt% [4]. Due to the complexity and particularity of the composition of laterite nickel ore, the Al$_2$O$_3$ content in the slag produced during the smelting process in the blast furnace is higher than 20wt% and may contain some Cr$_2$O$_3$, TiO$_2$, and MnO [5–7]. Increases in the Al$_2$O$_3$ content in slag can cause various problems, including slag stickiness, larger volumes of slag, and slag with a low desulfurization capacity [8]. The presence of Cr$_2$O$_3$ can further degrade slag fluidity because of its high melting point [6,9]. As the slag performance has a crucial influence on the smelting of laterite nickel ore in a blast furnace, it is important to study the performance of Cr$_2$O$_3$-bearing blast-furnace slag with a high Al$_2$O$_3$ content to ensure the stability and productivity of blast-furnace operations when smelting laterite nickel ore.

There have been many studies focused on the viscosity of high-Al$_2$O$_3$ slag, but relatively few related to the viscosity of high-Al$_2$O$_3$ slag containing Cr$_2$O$_3$. The effect of Al$_2$O$_3$ on the viscosity of CaO–SiO$_2$–Al$_2$O$_3$–9wt%MgO–1wt%TiO$_2$ (mass ratio of CaO/SiO$_2$ is 1.2) slag was studied by Yan *et al*. [10]. The authors found that the viscosity increased with increasing Al$_2$O$_3$ content in the range of 16wt% to 24wt% due to the polymerization of the aluminosilicate structures, followed by a decrease in viscosity in slags with Al$_2$O$_3$ contents higher than 24wt% due to its effect as a network modifier. Zhang *et al*. [11] studied the effect of Al$_2$O$_3$ on the viscosity of CaO–SiO$_2$–Al$_2$O$_3$–MgO–TiO$_2$–FeO blast-furnace slag with Al$_2$O$_3$ contents ranging from 14.84wt% to 23.84wt%. The authors found that the slag stability gradually worsens with increasing Al$_2$O$_3$ content due to the increasing degree of slag polymerization. In the study by Yao *et al*. [12], the viscosity

🙂 Springer

of high-alumina CaO–SiO$_2$–Al$_2$O$_3$–MgO blast-furnace slag was investigated, and the authors found that the slag viscosity could be increased despite higher Al$_2$O$_3$ contents at a fixed CaO/SiO$_2$ mass ratio of between 1.1 and 1.2. Kim *et al.* [13] investigated the effect of Al$_2$O$_3$ on the viscosity of CaO–SiO$_2$–Al$_2$O$_3$–10wt%MgO slag and proposed that a higher Al$_2$O$_3$ content could also increase the slag viscosity at a fixed CaO/SiO$_2$ mass ratio of between 0.8 and 1.3. The amphoteric behavior of Al$_2$O$_3$ in CaO–SiO$_2$(–MgO)–Al$_2$O$_3$ slag was investigated by Park *et al.* [14], who concluded that the viscosity increase by the influence of Al$_2$O$_3$ was due to the increase in the degree of polymerization and the incorporation of the [AlO$_4$]-tetrahedral into [SiO$_4$]-tetrahedral units, with the viscosity decrease attributable to the decrease in the degree of polymerization by the increasing relative fraction of [AlO$_6$]-octahedral units.

Due to the difficulty of measuring the high-temperature viscosity of slag, many empirical models have been developed to predict the viscosity of molten slag. Urbain's model [15] is based on the Weymann–Frenkel equation, with the slag components divided among glass formers, modifiers, and amphoterics. Similar to the basis of Urbain's model, Riboud's model [16] classifies slag components into five categories. The slag structure is associated with the modified basicity index (B_i^*) in Iida's model [17–18], based on the Arrhenius equation. The optical basicity model (NPL) [19–21] introduced the concept of modified optical basicity (Λ^{corr}) for calculating the parameters in the Arrhenius equation. Nakamoto's model [22–24] is based on non-bridging oxygen and free oxygen ions in the silicate structure. A structurally based viscosity model was proposed by Zhang *et al.* [25], by which various oxygen ions are classified to describe the slag structure based on the metal cations with which they have bonded.

To better understand the effect of Al$_2$O$_3$ on CaO–SiO$_2$–Al$_2$O$_3$–MgO–Cr$_2$O$_3$ slag, the viscosity of pentabasic slag was measured under the following conditions: mass ratio of CaO/SiO$_2$ is 1.0; contents of Al$_2$O$_3$, MgO, and Cr$_2$O$_3$ are 17wt%–29wt%, 8wt%, and 1wt%, respectively; high temperatures. The apparent activation energy was obtained to analyze the structure of the molten slag.

2. Experimental

2.1. Slag preparation

The samples were prepared using the analytical reagent-grade chemicals CaO, SiO$_2$, Al$_2$O$_3$, MgO, and Cr$_2$O$_3$, which were dried at 378 K for 12 h before use. The chemical compositions are listed in Table 1. The content of Al$_2$O$_3$ was increased from 17wt% to 29wt%, and the CaO/SiO$_2$ mass ratio was set to 1.0. Precisely weighted mixtures of 125 g were thoroughly mixed in an agate mortar and then were kept hermetically sealed for subsequent viscosity measurement.

Table 1.   Chemical compositions of the slags

Sample	Composition / wt%					Mass ratio of CaO/SiO$_2$
	CaO	SiO$_2$	Al$_2$O$_3$	MgO	Cr$_2$O$_3$	
No. 1	37.0	37.0	17.0	8.0	1.0	1.0
No. 2	35.5	35.5	20.0	8.0	1.0	1.0
No. 3	34.0	34.0	23.0	8.0	1.0	1.0
No. 4	32.5	32.5	26.0	8.0	1.0	1.0
No. 5	31.0	31.0	29.0	8.0	1.0	1.0

2.2. Experimental procedure of viscosity measurement

The slag viscosity was measured using the rotating cylinder method. As shown in Fig. 1, the experimental apparatus consisted of an RTW-10 viscometer connected to a molybdenum (Mo) spindle suspended on a Mo wire. The furnace temperature zone in the corundum tube (inner diameter = 53 mm) is strictly controlled by a computer program, with the temperature measured from 0 to 1873 K by a Pt–10%Rh/Pt thermocouple connected to the bottom of the Mo crucible. Before each measurement, analytical-reagent-grade castor oil with a known viscosity was used to regularly and precisely calibrate the viscometer.
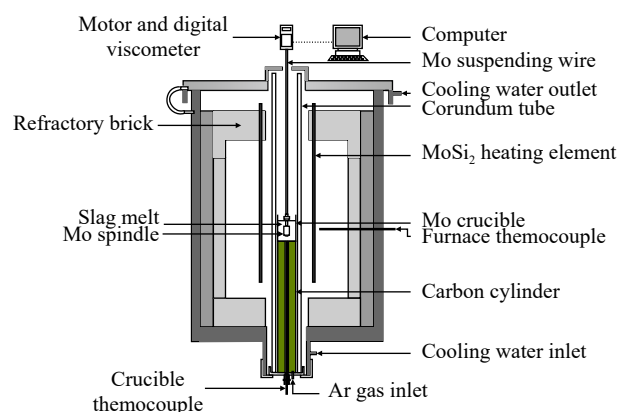

Fig. 1.   Experimental apparatus used to measure slag viscosity.

The blended slag sample was loaded into a Mo crucible (inner diameter = 39 mm and height = 60 mm), which was nested in a graphite crucible. The set of crucibles was placed inside the furnace temperature zone, and the furnace was heated from ambient temperature to 1823 K by the MoSi$_2$ heating element. To ensure the complete and homogeneous melting of the slag, the temperature was maintained at 1823 K for approximately 3 h. The furnace was then raised and the Mo spindle was immersed in the molten slag to approximately 7 mm from the bottom of the crucible, and the viscosity of the slag was then measured continuously after the Mo spindle began rotating steadily at a fixed rate of 200 r/min while cooling at a rate of 3 K/min. After the viscosity measurement, the slag was reheated to 1823 K for water quenching. Each measurement was performed in high-purity argon

atmosphere (99.999%, 1.0 L/min) to prevent oxidation of the Mo crucible and spindle during the measurement process. Some of the crucial measurements were repeated to confirm the reproducibility and reliability of the viscosity values.

3. Results and discussion

3.1. Effect of Al$_2$O$_3$ on the viscosity and critical temperature

In Fig. 2, the viscosities of the CaO–SiO$_2$–Al$_2$O$_3$–8wt%MgO–1wt%Cr$_2$O$_3$ slags with different Al$_2$O$_3$ contents are shown as a function of temperature. We can see that the viscosity of the molten slag gradually increases with decreases in temperature, and also increases with increases in the Al$_2$O$_3$ content. This indicates that Al$_2$O$_3$ continues to exist in the form of acidic oxides in this slag system, with the structure of the slag becoming complex and the migration resistance of the complex anion groups in the slag increasing with increasing Al$_2$O$_3$ content, thereby increasing the slag viscosity.
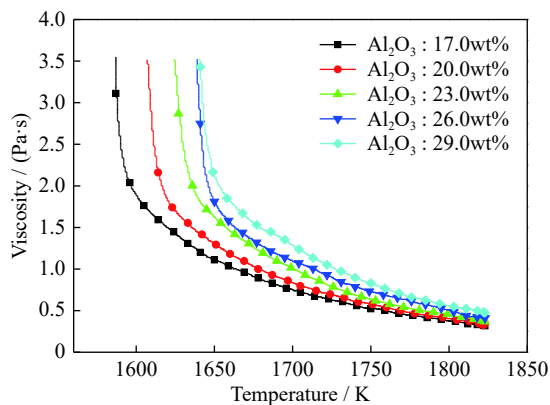
Fig. 2.   Viscosity of the CaO–SiO$_2$–Al$_2$O$_3$–8wt%MgO–1wt% Cr$_2$O$_3$ slag as a function of temperature with different Al$_2$O$_3$ contents.

Fig. 3 shows a graphic comparison of the viscosities of CaO–SiO$_2$–Al$_2$O$_3$–8wt%MgO–1wt%Cr$_2$O$_3$ (mass ratio of CaO/SiO$_2$ is 1.0) slag and CaO-SiO$_2$–Al$_2$O$_3$–9wt%MgO–1wt%TiO$_2$ (mass ratio of CaO/SiO$_2$ is 1.2) slag at different temperatures. Reported by Yan *et al*., the viscosity of the typical titanium-containing high-Al$_2$O$_3$ slag was to increase with the addition of Al$_2$O$_3$ up to 24wt%, then decrease with Al$_2$O$_3$ contents higher than 24wt% [10]. However, in this study, the slag viscosity increased gradually with increases in the Al$_2$O$_3$ content from 17wt% to 29wt%. This indicates that Al$_2$O$_3$ serves as a network former in the slag system.

The Cr$_2$O$_3$ in CaO–SiO$_2$–Al$_2$O$_3$–8wt%MgO–1wt%Cr$_2$O$_3$ slag has a high melting point. As shown in Fig. 4, increases in the Al$_2$O$_3$ content decreases the temperature of Cr$_2$O$_3$ precipitation. The generated solid phase has a greater effect on increasing the slag viscosity, such that the slag viscosity increases with increases in the Al$_2$O$_3$ content at high temperature. This means that Al$_2$O$_3$ has different mechanisms for influencing the properties of CaO–SiO$_2$–Al$_2$O$_3$–MgO slag and CaO–SiO$_2$–Al$_2$O$_3$–8wt%MgO–1wt%Cr$_2$O$_3$ slag. It also means that the presence of trace oxides in the slag results in the slag performance being affected by more influence factors and more complex influence mechanisms.
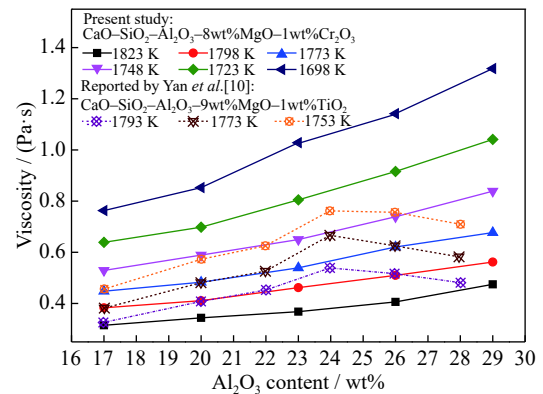
Fig. 3.   Effect of Al$_2$O$_3$ on the viscosity of CaO–SiO$_2$–Al$_2$O$_3$–8wt%MgO–1wt%Cr$_2$O$_3$ slag at different temperatures.
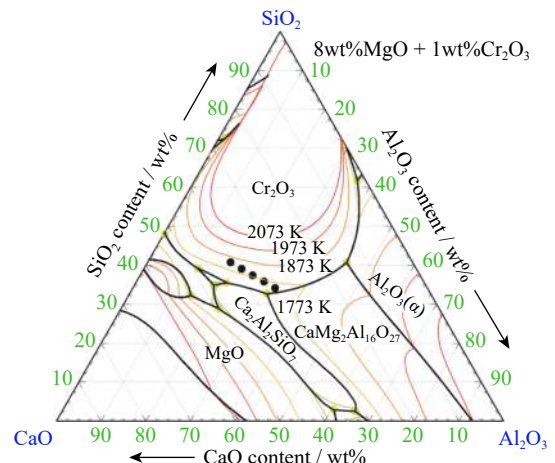
Fig. 4.   Phase diagram of the CaO–SiO$_2$–Al$_2$O$_3$–8wt%MgO–1wt%Cr$_2$O$_3$ slag system.

The critical temperature is the minimum temperature at which the fluidity of the molten slag experiences a sudden decrease, the slag exhibits non-Newtonian behavior, and the activation energy changes significantly [26–28]. This point is determined by the intersections of tangent lines with slopes equal to 1 on the viscosity–temperature curves shown in Fig. 2. As shown in Fig. 5, the critical temperature of CaO–SiO$_2$–Al$_2$O$_3$–8wt%MgO–1wt%Cr$_2$O$_3$ slag becomes higher from 1612 to 1668 K with increases in the Al$_2$O$_3$ content from 17wt% to 29wt%. Consequently, we can conclude that the critical temperature of CaO–SiO$_2$–Al$_2$O$_3$–8wt%MgO–1wt%Cr$_2$O$_3$ slag can be significantly affected by the addition of Al$_2$O$_3$, whereby the more is the Al$_2$O$_3$ content, the higher is the critical temperature. It also indicates that crystalline sub-

stances easily precipitate from the CaO–SiO$_2$–Al$_2$O$_3$–8wt% MgO–1wt%Cr$_2$O$_3$ slag, which causes the slag performance to be more unstable with increases in the Al$_2$O$_3$ content.
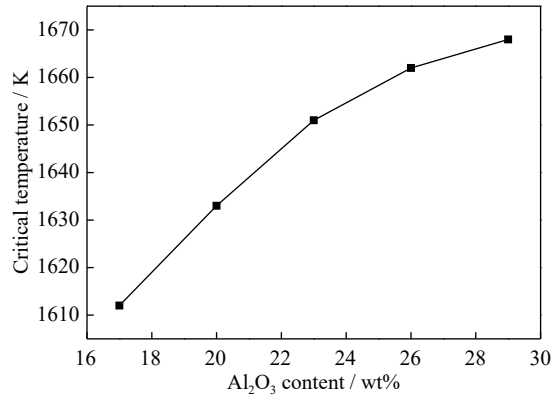

Fig. 5. **Effect of Al$_2$O$_3$ on the critical temperature of the CaO–SiO$_2$–Al$_2$O$_3$–8wt%MgO–1wt%Cr$_2$O$_3$ slag.**

3.2. Apparent activation energy for viscous flow

The viscosity of silicate melts can be expressed as a function of composition and temperature, which is correlated with the degree of polymerization. Variation in the activation energy can indicate the changes in frictional resistance to viscous flow, which reflect the change in the slag structure [29–30]. Assuming that the slag component remains constant during the experiment, the activation energy is considered to indicate the degree of polymerization, which can be obtained using the Arrhenius equation as follows:

$$\mu = A_0 \mathrm{e}^{(E_a/RT)} \tag{1}$$

where μ, A_0, E_a, R, and T are the viscosity, pre-exponent constant, apparent activation energy for viscous flow, universal gas constant, and absolute temperature (K), respectively. Hence, it is possible to obtain the apparent activation energy E_a by plotting $\ln\mu$ vs. $1/T$.

The Arrhenius plot for CaO–SiO$_2$–Al$_2$O$_3$–8wt%MgO–1wt%Cr$_2$O$_3$ slag is shown in Fig. 6 as a function of reciprocal temperature and the Al$_2$O$_3$ content. In the figure, we can see that $\ln\mu$ linearly increases with increases in $1/T$ in the Newtonian viscous flow region. The apparent activation energy is calculated based on the slopes of the lines in Fig. 6 and is listed in Table 2. It can be observed that E_a increases from 180.85 to 210.23 kJ/mol with increases in the Al$_2$O$_3$ content from 17wt% to 29wt%. The variation of the apparent activation energy with the Al$_2$O$_3$ content, as shown in Fig. 7, is very similar to the change in the critical temperature. This also indicates that the structure becomes complex and the degree of polymerization increases with increases in the Al$_2$O$_3$ content in CaO–SiO$_2$–Al$_2$O$_3$–8wt%MgO–1wt%Cr$_2$O$_3$ slag.

3.3. Effect of Al$_2$O$_3$ content on the structure

Fourier-transform infrared (FT-IR) spectroscopy was used
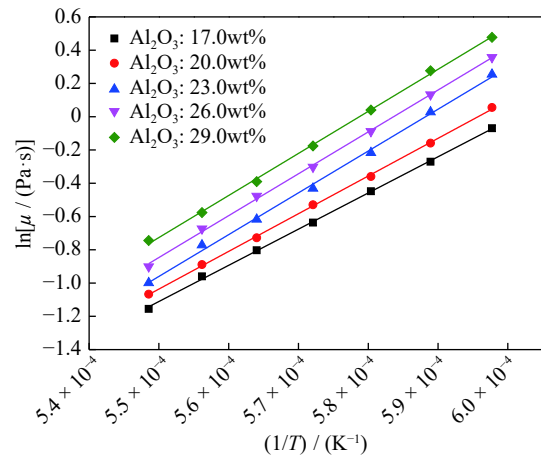
Fig. 6. **Arrhenius plot for CaO–SiO$_2$–Al$_2$O$_3$–8wt%MgO–1wt% Cr$_2$O$_3$ slag in the Newtonian flow region.**

Table 2. **Apparent activation energy of CaO–SiO$_2$–Al$_2$O$_3$–8wt% MgO–1wt%Cr$_2$O$_3$ slag**

Sample	Al$_2$O$_3$ content / wt%	E_a / (kJ·mol^{-1})
No.1	17.0	180.85
No.2	20.0	188.35
No.3	23.0	208.91
No.4	26.0	209.28
No.5	29.0	210.23
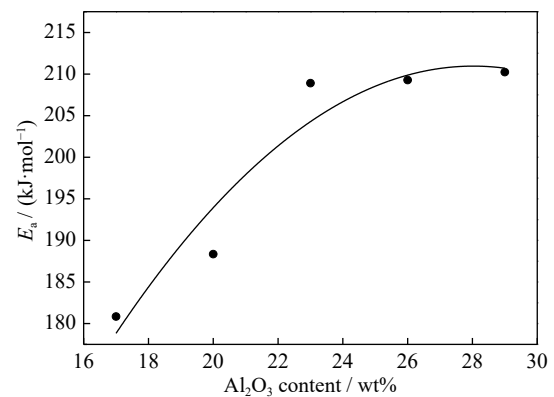
Fig. 7. **Effect of Al$_2$O$_3$ content on the apparent activation energy of CaO–SiO$_2$–Al$_2$O$_3$–8wt%MgO–1wt%Cr$_2$O$_3$ (mass ratio of CaO/SiO$_2$ is 1.0) slag.**

on the water-quenched slag to clarify the influence of Al$_2$O$_3$ on the slag structure, and Fig. 8 shows the results for CaO–SiO$_2$–Al$_2$O$_3$–8wt%MgO–1wt%Cr$_2$O$_3$ (mass ratio of CaO/SiO$_2$ is 1.0, and Al$_2$O$_3$ content is 20wt%–26wt%). As can be seen, the strong broad band from 1200 to 750 cm^{-1} is generally related to the symmetric stretching vibration of the [SiO$_4$]$^{4-}$ tetrahedral units, the weak band between 750 and 630 cm^{-1} is assigned to the asymmetric stretching vibration of the [AlO$_4$]$^{5-}$ tetrahedral units, and the band near 500 cm^{-1} is believed to be that of the [Si–O–Al] bending vibration. We can see that the bands for the [SiO$_4$]$^{4-}$ tetrahedral units be-

come deeper with increases in the Al$_2$O$_3$ content, whereas no major change is observed for the [AlO$_4$]$^{5-}$ tetrahedral units and [Si–O–Al] bending. Therefore, increases in the Al$_2$O$_3$ content in CaO–SiO$_2$–Al$_2$O$_3$–8wt%MgO–1wt%Cr$_2$O$_3$ slag increases the relative fraction of the [SiO$_4$]$^{4-}$ tetrahedral units, which increases the viscosity of the molten slag. Moreover, the peak valley of the [Si–O–Al] bending vibration moves to higher wavenumbers, which means that the distance between Si/Al and O becomes shorter, which indicates that the network structure is polymerized, as put forth by Badger's rule [31–32].
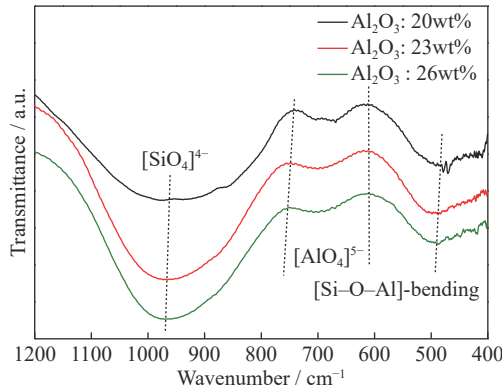

Fig. 8. FT-IR transmittance of CaO–SiO$_2$–Al$_2$O$_3$–8wt%MgO–1wt%Cr$_2$O$_3$ slag quenched from 1823 K.

3.4. Viscosity prediction of model

To predict the viscosity of CaO–SiO$_2$–Al$_2$O$_3$–8wt%MgO–1wt%Cr$_2$O$_3$ slag, we applied Iida's model due to the presence of Cr$_2$O$_3$, the expressions for which take the structure into consideration and are as follows:

$$\mu = A\mu_0 \, e^{E/B_i^*} \tag{2}$$

$$A = 1.745 - 1.962 \times 10^{-3}T + 7.000 \times 10^{-7}T^2 \tag{3}$$

$$E = 11.11 - 3.65 \times 10^{-3}T \tag{4}$$

where A and E are parameters determined based on standard reference material for high temperature and viscosity measurements, respectively, B_i^* is the modified basicity index, and μ_0 is the viscosity of non-network-forming melts, which can be approximately calculated using the following equations:

$$\mu_0 = \sum_{i=1}^{n} \mu_{0i} X_i \tag{5}$$

$$\mu_{0i} = 1.8 \times 10^{-7} \frac{[M_i(T_m)_i]^{1/2} e^{(H_i/RT)}}{(V_m)_i^{2/3} e^{[H_i/R(T_m)_i]}} \tag{6}$$

$$H_i \equiv 5.1(T_m)_i^{1/2} \tag{7}$$

where M is the formula weight, V_m is the molar volume at T_m, X is the mole fraction, and the subscript i represents the component. This model is related to the modified basicity index B_i^*, which can be expressed as follows:

$$B_i^* = \frac{\sum (\alpha_i W_i)_B + \alpha_{Fe_2O_3}^* W_{Fe_2O_3}}{\sum (\alpha_i W_i)_A + \alpha_{Al_2O_3}^* W_{Al_2O_3} + \alpha_{TiO_2}^* W_{TiO_2}} \tag{8}$$

where α is the specific coefficient, W is the mass percentage, the subscript A represents the acidic oxide, and the subscript B indicates the basic oxide or fluoride. α_i^* is a modified specific coefficient that can be expressed as a function of the slag component and temperature and indicates the interaction between the amphoteric oxide and other components in slags. The value for $\alpha_{Al_2O_3}^*$ in the CaO–SiO$_2$–Al$_2$O$_3$–MgO system was determined based on the measured viscosity data of 34 different slags [33–34], which can be expressed as follows:

$$\alpha_{Al_2O_3}^* = aB_i + bW_{Al_2O_3} + c \tag{9}$$

$$a = 1.20 \times 10^{-5}T^2 - 4.3552 \times 10^{-2}T + 41.16 \tag{10}$$

$$b = 1.40 \times 10^{-7}T^2 - 3.4944 \times 10^{-4}T + 0.2062 \tag{11}$$

$$c = -8.00 \times 10^{-6}T^2 + 2.5568 \times 10^{-2}T - 22.16 \tag{12}$$

where a, b, and c are the temperature-dependent coefficients.

Table 3 lists the values for α_i and μ_{0i}. The viscosities were then determined using Iida's model at the temperatures 1673, 1723, 1773, and 1803 K and compared with the measured viscosity data shown in Fig. 9. We determined the performance of the viscosity model using the following parameters:

Table 3.   Values of α_i and μ_{0i} for different oxides

Oxide		α_i	μ_{0i} / (mPa·s)			
			1673 K	1723 K	1773 K	1803 K
Acidic oxide	SiO$_2$	1.48	3.76	3.43	3.11	2.92
Amphoteric oxide	Al$_2$O$_3$	0.10	7.95	7.12	6.36	5.89
Basic oxide	CaO	1.53	23.82	20.67	17.83	16.15
	MgO	1.51	39.66	34.01	28.96	26.03
	Cr$_2$O$_3$	0.13	18.14	15.92	14.07	13.11

$$\delta = \frac{\mu_{cal} - \mu_{meas}}{\mu_{meas}} \times 100\% \tag{13}$$

$$\Delta = \frac{1}{N} \sum_{n=1}^{N} |\delta| \times 100\% \tag{14}$$

where μ_{cal} is the calculated viscosity, μ_{meas} is the measured viscosity, and N is the number of viscosity data. The parameters δ and Δ imply the relative difference between calculated and measured viscosities.

Table 4 shows the calculated δ and Δ values, which clarify the relative difference between the calculated and measured viscosities. It can be seen that the δ values generally increase with increases in the Al$_2$O$_3$ content in the CaO–SiO$_2$–Al$_2$O$_3$–8wt%MgO–1wt%Cr$_2$O$_3$ slag within the temperature range of 1673 to 1803 K. We can observe that the lower is the temperature, the better is the agreement between the calculated and measured viscosities, and the lower their deviation, as observed in Fig. 9. This indicates that the calculated vis-

Table 4. Values for δ and Δ obtained based on the calculated and measured viscosities of the $CaO-SiO_2-Al_2O_3-8wt\%MgO-1wt\%Cr_2O_3$ slags with the Al_2O_3 content from 17wt% to 29wt%

Temperature / K	δ / %					Δ / %
	17wt%*	20wt%*	23wt%*	26wt%*	29wt%*	
1673	−16.1	−13.6	−15.7	−2.9	5.8	10.8
1723	−30.5	−31.0	−34.2	−35.2	−34.5	33.1
1773	−40.0	−43.2	−47.5	−52.7	−53.3	47.3
1803	−45.3	−49.2	−53.9	−58.0	−61.5	53.6

Note: * menas the Al_2O_3 content in the slag
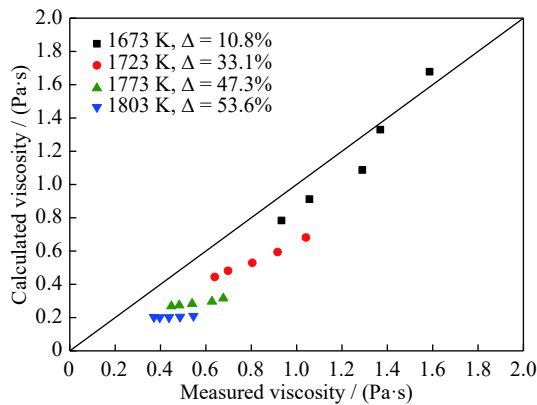
Fig. 9. Comparison of measured viscosity with the viscosity calculated using Iida's model.

cosity values obtained using Iida's model conform best to the measured values when both the temperature and Al_2O_3 content are at relatively low levels, i.e., within the temperature range of 1673 to 1803 K and the Al_2O_3 content range of 17wt%–29wt% in $CaO-SiO_2-Al_2O_3-8wt\%MgO-1wt\%Cr_2O_3$ slag.

4. Conclusions

The viscosity of $CaO-SiO_2-Al_2O_3-8wt\%MgO-1wt\%Cr_2O_3$ (mass ratio of CaO/SiO_2 is 1.0, Al_2O_3 content is 17wt%–29wt%) slag was experimentally measured to determine the effect of Al_2O_3 content on the behavior of penta-basic slag formed mainly in a blast furnace when smelting laterite nickel ore. The apparent activation energy was obtained to clarify the role of Al_2O_3 in changing the structure of the molten slag. Iida's model was used to predict the viscosity relative to the content of Cr_2O_3 in the slag. Our conclusions are summarized as follows.

(1) The viscosity increases gradually with increases in the Al_2O_3 content within the range of 17wt%–29wt%. The critical temperature also increases from 1612 to 1668 K with increases in the Al_2O_3 content from 17wt%–29wt%.

(2) The apparent activation energy increases from 180.85 to 210.23 kJ/mol with increases in the Al_2O_3 content from 17wt% to 29wt%, which is consistent with the variation of the critical temperature. This indicates that the structure be-

comes complex and the degree of polymerization increases.

(3) The FT-IR spectra obtained for the water-quenched slag indicate that the slag structure becomes polymerized with increases in the relative fraction of $[SiO_4]^{4-}$ tetrahedral units and the higher wavenumbers of the peak valleys of the [Si–O–Al] bending vibration.

(4) Iida's model can be applied to predict the viscosity of $CaO-SiO_2-Al_2O_3-8wt\%MgO-1wt\%Cr_2O_3$ (mass ratio of CaO/SiO_2 is 1.0, and Al_2O_3 content is 17wt%–29wt%) slag within the temperature range of 1673 to 1803 K. Moreover, the better consistency between the calculated viscosity and measured one can be obtained with lower temperature and/or fewer Al_2O_3 content.

References

[1] J.H. Li, X.H. Li, Q.Y. Hu, Z.X. Wang, Y.Y. Zhou, J.C. Zheng, W.R. Liu, and L.J. Li, Effect of pre-roasting on leaching of laterite, *Hydrometallurgy*, 99(2009), No. 1-2, p. 84.

[2] T. Norgate and S. Jahanshahi, Assessing the energy and greenhouse gas footprints of nickel laterite processing, *Miner. Eng.*, 24(2011), No. 7, p. 698.

[3] B.S. Zhang, K.X. Jiang, H.B. Wang, and Y.P. Feng, Progress of pyrometallurgical smelting technologies for laterite nickel ore in China, *Nonferrous Met. Eng. Res.*, 33(2012), No. 5, p. 16.

[4] Y.P. Zhang, Technico-economical analysis of Ni-containing hot metal production with laterite in the blast furnace, *Ferro-Alloys*, 44(2013), No. 4, p. 10.

[5] R.Z. Xu, J.L. Zhang, X.Y. Fan, W.W. Zheng, and Y.A. Zhao, Effect of MnO on high-alumina slag viscosity and corrosion behavior of refractory in slags, *ISIJ Int.*, 57(2017), No. 11, p. 1887.

[6] R.Z. Xu, J.L. Zhang, Z.Y. Wang, and K.X. Jiao, Influence of Cr_2O_3 and B_2O_3 on viscosity and structure of high alumina slag, *Steel Res. Int.*, 88(2017), No. 4, art. No. 1600241.

[7] R.Z. Xu, J.L. Zhang, R.Y. Ma, K.X. Jiao, and Y.A. Zhao, Influence of TiO_2 on the viscosity of a high alumina slag and on carbon brick corrosion, *Steel Res. Int.*, 89(2018), No. 3, art. No. 1700353.

[8] C.K. Du, J. Yang, X.Z. Zhao, Y.J. Shi, J.L. You, and X.D. Gao,

Viscosity and desulfurization behavior of blast furnace slag with high Al$_2$O$_3$ content, *J. Iron Steel Res.*, 25(2013), No. 7, p. 19.

[9] J. Ma, G.Q. Fu, W. Li, and M.Y. Zhu, Influence of TiO$_2$ on the melting property and viscosity of Cr-containing high-Ti melting slag, *Int. J. Miner. Metall. Mater.*, 27(2020), No. 3, p. 310.

[10] Z.M. Yan, X.W. Lv, D. Liang J. Zhang, and C.G. Bai, Transition of blast furnace slag from silicates-based to aluminates-based: Viscosity, *Metall. Mater. Trans. B*, 48(2017), No. 2, p. 1092.

[11] X.F. Zhang, T. Jiang, X.X. Xue, and B.S. Hu, Influence of MgO/Al$_2$O$_3$ ratio on viscosity of blast furnace slag with high Al$_2$O$_3$ content, *Steel Res. Int.*, 87(2016), No. 1, p. 87.

[12] L. Yao, S. Ren, X.Q. Wang, Q.C. Liu, L.Y. Dong, J.F. Yang, and J.B. Liu, Effect of Al$_2$O$_3$, MgO and CaO/SiO$_2$ on viscosity of high alumina blast furnace slag, *Steel Res. Int.*, 87(2016), No. 2, p. 241.

[13] H. Kim, H. Matsuura, F. Tsukihashi, W.L. Wang, D.J. Min, and I. Sohn, Effect of Al$_2$O$_3$ and CaO/SiO$_2$ on the viscosity of calcium-silicate–based slags containing 10 mass pct MgO, *Metall. Mater. Trans. B*, 44(2013), No. 1, p. 5.

[14] J.H. Park, D.J. Min, and H.S. Song, Amphoteric behavior of alumina in viscous flow and structure of CaO–SiO$_2$(–MgO)–Al$_2$O$_3$ slags, *Metall. Mater. Trans. B*, 35(2004), No. 2, p. 269.

[15] G. Urbain, Viscosity estimation of slags, *Steel Res. Int.*, 58(1987), No. 3, p. 111.

[16] P.V. Riboud, Y. Roux, L.D. Lucas, and H. Gaye, Improvement of continuous casting powders, *Fachber. Hüttenprax. Metallweiterverarbei.*, 19(1981), No. 10, p. 859.

[17] T. Iida, H. Sakai, Y. Kita, and K. Murakami, Equation for estimating viscosities of industrial mold fluxes, *High Temp. Mater. Processes*, 19(2000), No. 3-4, p. 153.

[18] T. Iida, H. Sakai, Y. Kita, and K. Shigeno, An equation for accurate prediction of the viscosities of blast furnace type slags from chemical composition, *ISIJ Int.*, 40(2000), p. S110.

[19] K.C. Mills and S. Sridhar, Viscosities of ironmaking and steelmaking slags, *Ironmaking Steelmaking*, 26(1999), No. 4, p. 262.

[20] H.S. Ray and S. Pal, Simple method for theoretical estimation of viscosity of oxide melts using optical basicity, *Ironmaking Steelmaking*, 31(2004), No. 2, p. 125.

[21] A. Shankar, M. Görnerup, A.K. Lahiri, and S. Seetharaman, Estimation of viscosity for blast furnace type slags, *Ironmaking Steelmaking*, 34(2007), No. 6, p. 477.

[22] M. Nakamoto, J. Lee, and T. Tanaka, A model for estimation of viscosity of molten silicate slag, *ISIJ Int.*, 45(2005), No. 5, p. 651.

[23] M. Nakamoto, Y. Miyabayashi, L. Holappa, and T. Tanaka, A model for estimating viscosities of aluminosilicate melts containing alkali oxides, *ISIJ Int.*, 47(2007), No. 10, p. 1409.

[24] Y. Miyabayashi, M. Nakamoto, T. Tanaka, and T. Yamamoto, A model for estimating the viscosity of molten aluminosilicate containing calcium fluoride, *ISIJ Int.*, 49(2009), No. 3, p. 343.

[25] G.H. Zhang, K.C. Chou, and K. Mills, A structurally based viscosity model for oxide melts, *Metall. Mater. Trans. B*, 45(2014), No. 2, p. 698.

[26] G.B. Qiu, L. Chen, J.Y. Zhu, X.W. Lv, and C.G. Bai, Effect of Cr$_2$O$_3$ addition on viscosity and structure of Ti-bearing blast furnace slag, *ISIJ Int.*, 55(2015), No. 7, p. 1367.

[27] J.H. Park, D.J. Min, and H.S. Song, The effect of CaF$_2$ on the viscosities and structures of CaO–SiO$_2$(–MgO)–CaF$_2$ slags, *Metall. Mater. Trans. B*, 33(2002), No. 5, p. 723.

[28] C. Wang, J.L Zhang, Z.J. Liu, K.X. Jiao, G.W. Wang, J.Q. Yang, and K.C. Chou, Effect of chlorine on the viscosities and structures of CaO–SiO$_2$–CaCl$_2$ slags, *Metall. Mater. Trans. B*, 48(2017), No. 1, p. 328.

[29] K.Y. Ko and J.H. Park, Effect of CaF$_2$ addition on the viscosity and structure of CaO–SiO$_2$–MnO slags, *ISIJ Int.*, 53(2013), No. 6, p. 958.

[30] J.H. Park, Structure-property correlations of CaO–SiO$_2$–MnO slag derived from Raman spectroscopy, *ISIJ Int.*, 52(2012), No. 9, p. 1627.

[31] J.H. Park, D.J. Min, and H.S. Song, Structural investigation of CaO–Al$_2$O$_3$ and CaO–Al$_2$O$_3$–CaF$_2$ slags via fourier transform infrared spectra, *ISIJ Int.*, 42(2002), No. 1, p. 38.

[32] W.H. Kim, I. Sohn, and D.J. Min, A study on the viscous behaviour with K$_2$O additions in the CaO–SiO$_2$–Al$_2$O$_3$–MgO–K$_2$O quinary slag system, *Steel Res. Int.*, 81(2010), No. 9, p. 735.

[33] J.S. Machin, T.B. Yee, and D.L. Hanna, Viscosity studies of system CaO–MgO–Al$_2$O$_3$–SiO$_2$: III, 35, 45, and 50% SiO$_2$, *J. Am. Ceram. Soc.*, 35(1952), No. 12, p. 322.

[34] J.S. Machin and D.L Hanna, Viscosity studies of system CaO–MgO–Al$_2$O$_3$–SiO$_2$: Ⅰ, 40% SiO$_2$, *J. Am. Ceram. Soc.*, 28(1945), No. 11, p. 310.